The interaction of water and hydrogen with nickel surfaces

Shan, J.

Chapter 5

Identification of Hydroxyl on Ni(111)

Hydroxyl (OH) is identified and characterized on the Ni(111) surface with high resolution electron energy loss spectroscopy. We find clear evidence of stretching, bending and translational modes that differ significantly from modes observed for H_2O and O on Ni(111). Hydroxyl may be produced from water using two different methods. Annealing of water co-adsorbed with atomic oxygen at 85 K to above 170 K leads to creation of OH with simultaneous desorption of excess water. Pure water layers treated in the same fashion show no dissociation. However, exposure of pure water to 20 eV electrons below 120 K produces OH in the presence of adsorbed H_2O. In combination with temperature-programmed desorption studies, we show that OH groups recombine between 180 and 240 K to form O and immediately desorbing H_2O. The lack of influence of co-adsorbed H_2O at 85 K on the hydroxyl's O-H stretching mode indicates that OH does not participate in a hydrogen-bond network.

5.1 Introduction

Hydroxyl adsorbed on metal surfaces (OH) has attracted much attention in recent years [1-10]. This is not surprising considering the central role of OH as a reaction intermediate in many heterogeneously catalyzed and electrochemical reactions. Despite considerable efforts, understanding of the formation and reaction pathways and the geometry of adsorbed OH, including its dependence on surface structure and co-adsorbates, remains limited.

Fisher and Sexton were the first to demonstrate formation of OH on a metal single crystal by means of high resolution electron energy loss spectroscopy (HREELS) and ultraviolet photoelectron spectroscopy (UPS) [1]. Annealing of water molecules adsorbed on oxygen pre-covered Pt(111) produced OH above 155 K. Formation of OH from the H_2O + O reaction on this surface was confirmed later by other groups employing various techniques [2,3], whereas water adsorption on clean Pt(111) is non-dissociative [11,12]. Besides the possibility of creating OH from co-adsorbed water and atomic oxygen, Mitchell and White reported OH production in an intermediate stage of the catalytic H_2 oxidation by O_2 on Pt(111) [4], although they noticed differences when comparing their HREEL spectra with Fisher and Sexton's. Later, Germer and Ho also observed OH during the H_2 oxidation by means of time-resolved EELS [5]. Their EEL spectra were more consistent with Fisher and Sexton's. Recently, discrepancies between these studies were explained by Ertl and co-authors [2]. They investigated the properties of OH on Pt(111) by means of HREELS and scanning tunneling microscopy (STM). In their studies, the properties and formation of OH under these two different reaction conditions were both studied and compared. Discrepancies between earlier studies were explained by the different degree of order under the different reaction conditions used to produce OH. Although such studies have shed light on the formation of OH on Pt(111), controversies persist. For example, HREELS studies have suggested that the adsorption site of OH is the three-fold hollow site [4,13], while STM, HREELS, low energy electron diffraction (LEED), and density functional theory (DFT) studies suggest preference for the top site [2,3].

Since the early studies by Fisher and Sexton, adsorbed OH has been identified on several other metal surfaces, e.g. Pd(100) [14], Si(100) [15], Ni(110) [16,17] most often by HREELS. Oddly, OH has not yet been identified on Ni(111), which is the dominating

surface structure on nickel catalyst particles. Adsorbed OH on this surface is therefore expected to be relevant to large industrial processes, such as methane steam reforming, but also to small scale applications, such as alkaline fuel cells. To date, spectroscopic studies for co-adsorption of H_2O with O on Ni(111) are inconsistent. From temperature programmed desorption (TPD) studies, Madey and Netzer suggested formation of OH as a result of annealing co-adsorbed H_2O+O above 120 K [6], whereas UPS studies by Pache *et al.* conclude that no OH forms under the same conditions [18]. Both suggestions were supported by later studies using reflection-adsorption infrared spectroscopy (RAIRS) [10], combined TPD and UPS [19], and TPD and X-ray photoelectron spectroscopy (XPS) [20]. Clear and unambiguous identification of OH on Ni(111) is currently lacking. Theoretical studies for OH on Ni(111) have so far focused on adsorption energy, site and geometry, concluding that OH is preferentially adsorbed on the three-fold hollow site with its O-H axis almost perpendicular to the surface [7,9,21].

In this Chapter, we use HREELS, Auger Electron Spectroscopy (AES) and TPD to study a single H_2O layer and H_2O co-adsorbed with O on Ni(111). We focus our attention on spectroscopic identification of species that are present before and after annealing these systems to various temperatures. Additionally, we have used electron bombardment of the pure H_2O layer to help us identify reaction products.

5.2 Experimental

Experiments are carried out in an UHV system, which consists of two chambers. The top chamber is equipped with an ion sputter gun, an atomic hydrogen source, a bakeable UHV leak valve, a movable tungsten filament, a home-built capillary array doser [22], and a quadrupole mass spectrometer (Balzers QMS 422) used for TPD measurement and residual gas analysis. The lower chamber contains an upgraded ELS 22 high resolution electron energy loss spectrometer and a double-pass CMA Auger electron spectrometer (Staib Instruments). The top and lower chambers are separated by a gate valve. The typical base pressure of the system is less than 1×10^{-10} mbar.

The Ni(111) single crystal, cut and polished to less than 0.1º of the low Miller-index plane (Surface Preparation Laboratories, Zaandam, the Netherlands), can be heated to 1200

K by electron bombardment and cooled to 85 K. The crystal temperature is measured by a chromel-alumel thermocouple spot-welded to the edge of the crystal. The crystal is cleaned by Ar^+ sputtering, annealing at 1100 K, followed by oxidation in 10^{-7} mbar of O_2 and reduction in 10^{-6} mbar of H_2. After cleaning, the surface cleanliness is verified by AES. H_2O (18.2 MΩ/cm resistance) is cleaned by repeated freeze-pump-thaw cycles after which helium (Messer, 99.999%) is introduced to the glass water container to a total pressure of approximately 1 bar. To increase water dosing accuracy, we monitor the helium partial pressure in the vacuum chamber when dosing water. H_2O is dosed through the capillary array doser, which is placed 15 mm in front of the sample. Water coverages are estimated from integrated TPD traces. A detailed description of our conversion of a TPD integral to absolute water coverage is presented in Chapter 3 or Ref 23. Atomic oxygen on the surface is produced from dissociative adsorption of O_2 [24], which we dose through the leak valve. The oxygen coverage is estimated using AES. In particular, we use the integrated AES feature near 513 eV for a 0.25 ML O-coverage from O_2 dissociation as a reference [10,25,26] when determining smaller O-coverages for the same integrated feature. All TPD measurements were performed with a heating rate of 1.0 K/s. The HREEL spectra were recorded at 5 to 9 meV resolution (FWHM) with typical 1×10^4 cps for the scattered elastic peak.

5.3 Results and Discussion

5.3.1 TPD Spectra

Figure 5.1 displays a set of TPD spectra of H_2O on clean and oxygen pre-dosed Ni(111). The sample temperature was kept at 85 K while dosing H_2O through the capillary array doser. Trace 5.1A is a TPD spectrum of H_2O desorption from clean Ni(111) without additional treatment. Trace 5.1B shows the TPD spectrum of H_2O desorption from the ~0.05 ML atomic oxygen pre-covered surface. In trace 5.1C, H_2O is adsorbed on the clean surface at 85 K before exposing the front of the crystal to 20 eV electrons for 100 s. Electrons are created by heating the moveable tungsten filament while acceleration of electrons toward the crystal is achieved by applying a potential of +20 eV to the crystal relative to the grounded filament. During electron bombardment, the crystal temperature

increases to ~120 K. The electron beam current is ~0.1 mA. After exposure to electrons, the crystal is cooled to 85 K before taking a TPD spectrum.

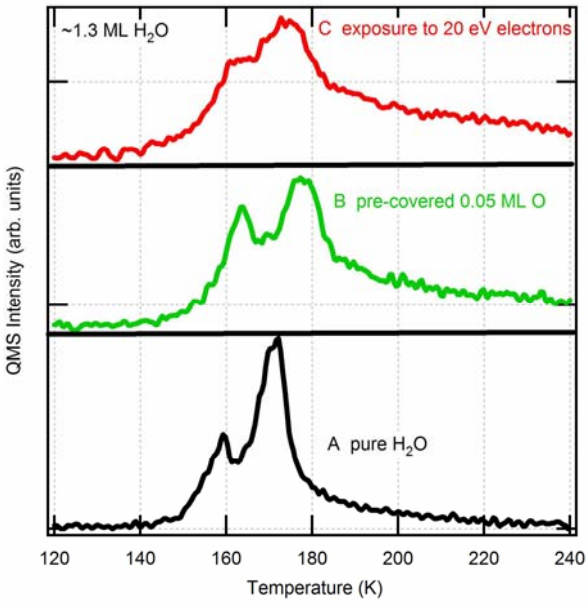

Figure 5.1 TPD of ~ 1.3 ML H_2O on clean and atomic oxygen pre-covered Ni(111) surface.

First, we focus on the trace 5.1A. The spectrum clearly shows two distinct desorption features: a high temperature peak at ~ 170 K and a low temperature peak at ~ 160 K. Such spectra corresponding to water desorption from clean Ni(111) have already been studied in detail before [6,18,19,23,27,28]. It is generally agreed that the high temperature peak is due to desorption from a (sub-)monolayer coverage of water interacting directly with the Ni(111) surface. The low temperature peak is due to desorption of multilayers of water. With increasing coverage, the (sub-)monolayer peak reaches saturation, while the multilayer peak does not saturate. For clarity, we only show a desorption trace of ~1.3 ML H_2O here. More traces with a wide coverage range can be found in Chapter 3 and 4.

In trace 5.1B desorption of H_2O from oxygen pre-covered Ni(111) shows two clear desorption features and a broad tail at higher temperatures, as observed previously by other groups [6,18,20]. These early studies ascribe the feature at ~ 162 K to desorption of water multilayers, while the feature at ~ 176 K is attributed to the (sub)monolayer desorption. The

observed shift from 170 to 176 K for this peak has generally been attributed to an increase in bond energy for water adsorbed to the surface when co-adsorbed with atomic oxygen. We observe a third, broad feature reaching up to above 240 K. It is generally described as occurring between ~ 180 K and ~ 240 K [6,18,20]. Two interpretations have been proposed for the appearance of this broad peak. The first interpretation suggests initial OH formation from reaction of H_2O + O with, at higher temperatures, reaction in the reverse direction [6,19]. The second interpretation attributes this feature to intact H_2O molecules directly chemisorbed on the Ni(111) surface [16,20]. Here, the new higher temperature feature was suggested to result from varying bond energies and differing H_2O-H_2O interactions.

Trace 5.1C shows three features which are very similar to those in the middle spectrum. Most prominently, the impact of electrons on the pure H_2O surface results in the same additional high temperature desorption feature between 180 and 240 K observed when co-adsorbing the same amount of water with ~0.05 ML atomic oxygen.

It is well known that energetic electrons impacting onto adsorbed water molecules may lead to dissociation of water into OH_{ads} and H_{ads} [29,30]. Also, TPD studies of recombination of OH on metal surfaces e.g. Pt(111) [1], Pt(110) [31], Pd(110) [32], show an additional high temperature desorption feature above 200 K [11,12]. The presence of the high temperature feature in TPD spectra 5.1B and 5.1C then suggests which of the two proposed origins for the broad high temperature feature is most likely: Co-adsorption with atomic oxygen, similar to impacting electrons, leads to formation of OH with consecutive recombination of OH to form H_2O and O between 180 and 240 K. To test this suggestion more stringently, we study the changes in vibrational features observed at various conditions and treatments in the next section. In this study, we do not pay particular attention to the H_{ads} created by electron impact. It may desorb instantaneously, recombine with OH_{ads} to form H_2O in competition with reaction between two adsorbed hydroxyl groups to form H_2O + O_{ads}, recombine with O_{ads} if the latter is formed from reaction between hydroxyl groups, or desorb as H_2 at higher temperatures.

5.3.3 Vibrational Spectra

HREEL spectra of ~1.1 ML H_2O adsorbed on Ni(111) pre-covered by ~0.05 ML atomic oxygen are shown in Figure 5.2 with various amplified regions. All spectra were recorded

at the specular angle with an impact energy of 5.0 eV. Trace 5.2A is a spectrum taken directly after preparing the system at 85 K. For trace 5.2B, we have annealed the system to 150 K for 100 s, followed by cooling to 85 K prior to collecting the spectrum. For trace 5.2C, we again annealed the same system for 100 s, but at the increased temperature of 170 K, followed by cooling to 85 K. Finally, for trace 5.2D, we have annealed the sample to 250 K for 100 s, followed by cooling. Annealing to 155 K in the first step leads to no changes compared to annealing to 150 K. When omitting the first annealing step and proceeding directly to annealing the system to 170 K, the same HREEL spectrum appears as shown in trace 5.2C. Changing the atomic oxygen pre-coverage to approximately 0.25 ML, while keeping the water coverage and annealing-cooling procedures the same, does also not result in any significant changes when compared to the HREEL spectra shown in Figure 5.2.

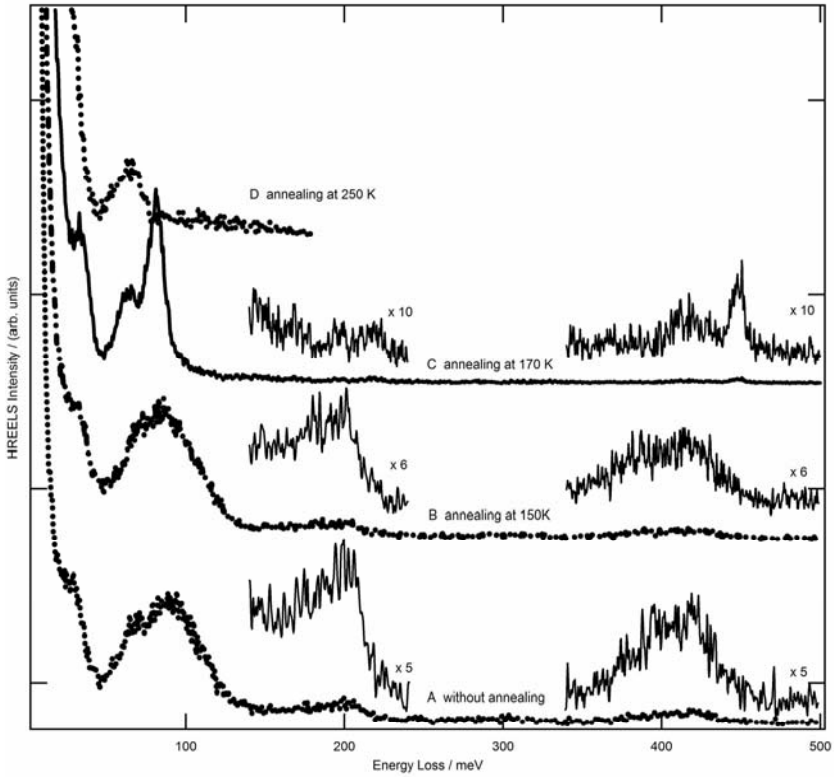

Figure 5.2 HREEL spectra of 1.1 ML H_2O co-adsorbed with ~0.05 ML atomic oxygen on Ni(111), followed by various annealing procedures.

In trace 5.2A, there are four distinct features, centered near 30, 90, 200, and 420 meV. The spectrum strongly resembles the spectrum of a comparable amount of H_2O adsorbed on clean Ni(111), showing the same positions and shapes of these features. A detailed analysis of the HREEL spectrum for H_2O/Ni(111) can be found in Chapter 3 and 4. In accordance with earlier assignments, we ascribe the 30 meV feature to H_2O's frustrated translation normal to the surface in a second or higher water layer. These H_2O molecules are hydrogen-bound to water molecules in lower layers, resulting in a (nearly) surface-independent frequency. The broad feature centered at 90 meV is ascribed to the librational modes of H_2O, which we can not resolve. The 200 meV feature is ascribed to the H-O-H bending mode. Finally, the 420 meV feature results from the O-H stretch mode in a hydrogen-bonded network. The shoulder near 70 meV on the low energy side of the 90 meV feature is most likely due to the Ni-O stretch. HREEL spectra of atomic oxygen on Ni(111) have previously identified this vibration at 70 meV [26,30]. We therefore conclude that spectrum A is the combined spectrum of O_{ads} and H_2O_{ads} and shows no additional features that may be related to formation of OH or other new species on the surface resulting from co-adsorption at 85 K. On Pt(111), the same conclusion was drawn for a similarly prepared system [1].

Trace 5.2B shows that annealing the O + H_2O layer on Ni(111) to 150 K (not shown is the same trace at lower resolution for 155 K) does not result in any significant changes. The four peaks described previously still occur at the same energies and with the same relative intensities. No new features appear. In contradiction to previous investigations that claim formation of OH near 120 K from H_2O + O on the basis of TPD and electron simulated desorption ion angular distribution (ESDIAD) techniques [6], we find no vibrational spectroscopic evidence for such reaction up to 155 K.

Trace 5.2C indicates that annealing to 170 K does result in significant changes in the species present on the Ni(111) surface. First, we find that features at 420 and 200 meV have (almost) entirely disappeared. A new, sharp feature appears at 450 meV. Also, the broad feature centered at 90 meV has been replaced by a much sharper and more intense feature centered at 83 meV. The shoulder peak observed near 70 meV in traces 5.2A and 5.2B now

appears more pronounced at 65 meV. Finally, careful inspection of the peak at the lowest energy indicates a shift from 30 meV in trace A and B to 34 meV in trace 5.2C.

Annealing to 250 K leads to a loss of all characteristic vibrational features except the feature around 65-70 meV, previously identified as the Ni-O stretch. We only show the highest resolution spectrum, which focuses on the regime up to 180 meV. Spectra taken at lower resolution over the entire energy range show no vibrational losses at higher energy.

First, we discuss the presence of water on the surface using both TPD and HREEL spectra from figures 5.1 and 5.2. In the vibrational spectra 5.2A and 5.2B, H_2O's characteristic stretching and bending frequencies at 420 and 200 meV are clearly present. TPD trace 5.1B shows that H_2O multilayers are not expected to desorb rapidly at 150 K and the continued presence of some multilayered water is confirmed by the H_2O-H_2O frustrated translational mode at 30 meV in trace 5.2B. In short, annealing to 150 K for 100 s does not affect the system as prepared.

Desorption of water occurs when annealing at higher temperatures. Multilayered water desorbs most rapidly near 160 K for this coverage. Monolayer desorption likely has an onset near the same temperature, but the convolution of desorption peaks in trace 5.1B renders us unable to identify a unique onset for such desorption. The large differences in the vibrational spectra shown in 5.2B and 5.2C strongly suggest that the chemical identity of species on the surface has also changed after annealing to 170 K. However, trace 5.1B shows that H_2O is still being produced at much higher temperatures. It appears that annealing ~1 ML H_2O co-adsorbed with ~0.05 ML O_{ads} to 170 K results in partial desorption of H_2O with a simultaneous chemical change at the surface that continues to yield water desorption at higher temperatures. From trace 5.2D, we conclude that, upon complete desorption of H_2O, adsorbed oxygen atoms remain.

The vibrational features in trace 5.2C shed light on the identity of the species present after annealing to 170 K. Starting with the highest energy loss, we note that the narrow peak appearing at 450 meV on Ni(111) is very close to the non-hydrogen-bonded O-H stretching frequency generally observed in a water network (around 458 meV) [34,35]. However, two arguments contest the assignment of this feature to non-hydrogen-bonded water. First, the appearance of this feature is not accompanied by an energy loss in the

regime for H-O-H bending vibrations. It seems very unlikely that the significant intensity of the stretch vibration could be associated with little or negilible intensity for the accompanying bending vibration. Second, in Chapter 4 we have found that in a regime where water coexist on the Ni(111) surface as a condensed phase and a lattice gas, the lattice gas shows a very strong and characteristic energy loss at 105 meV. This feature is clearly present in all spectra when non-hydrogen-bonded water molecules can coexist with hydrogen-bonded colleagues, but is not present in trace 5.2C. For these reasons we find it unlikely that the sharp feature at 450 meV results from intact water molecules bound in some way to the nickel lattice with an additional presence of 0.05 ML oxygen.

Adsorbed OH is a more likely the origin of the observed energy loss at 450 meV and the other changes observed between spectra 5.2B and 5.2C. First, the O-H stretching frequency is reported at 450 meV for free OH radicals [36]. As non-hydrogen-bonded OH, hydroxyl's stretch frequency appears at similar frequencies on Si(100) (463 meV) [15], and Pt(111) (456 meV) [37]. We note that the stretch frequency for OH in $\beta Ni(OH)_2$ has also been observed around 460 meV by inelastic neutron scattering (INS) [38]. Second, a bending frequency in the vicinity of 200 meV would not be expected for OH. We also do not observe a feature near this frequency. Instead, we observe a strong feature at 83 meV, which is reminiscent of the OH-bending frequency reported for OH on Ni(110) at 84 meV [17]. Finally, the appearance of a feature at 34 meV is consistent with the hindered translational modes of OH. On Pt(111) two separate features appear at 43 and 29 meV [2]. In trace 5.2C, this particular feature cannot result from multilayered water as TPD trace 5.1B indicates that multilayers have desorbed after annealing to 170 K. Our observation of a single mode instead of two on Pt(111) may result from our poorer resolution.

Considering the possible geometries for OH on a surface, a number of point groups and corresponding dipole active modes may be identified [39]. For an OH molecule adsorbed with its axis strictly along the surface normal point groups e.g. C_{6v}, C_{3v} and C_{2v} may be possible. However, such geometries are not very likely as OH is known to strongly tilt away from the surface normal on Pt(111) [2,3], and theoretical investigations for OH on Ni(111) predict a tilted geometry [7, 9, 21] with a 10º difference between the O-H bond axis and surface normal [7]. The reduced symmetry leads to point group C_S for OH

adsorbed on the three-fold hollow, the bridge and top sites if the symmetry plane for the O-H group is also a symmetry plane of the bare surface. For C_S, four dipole active modes and two impact scattering modes are expected. The dipole active modes may be described as the O-H stretch, Ni-OH stretch, OH rotation within the symmetry plane and OH translation within the symmetry plane. The impact scattering modes are the OH rotation and OH translation normal to the symmetry plane and are expected to be considerably less intense than the dipole active modes. Figure 5.3 presents an HREEL spectrum (C') taken at 10º from the specular angle. The spectrum was taken after the same treatment of the H_2O + O overlayer corresponding to spectrum C in figure 5.2. For comparison we repeat this spectrum in figure 5.3. We notice that all four peaks located near 450, 83, 65, and 34 meV, which only appear after annealing this overlayer, are dipole active. This observation strongly supports our attribution of the new peaks to hydroxyl groups. Considering the previous comparison to published spectra, the observed dipole activity allows us to identify the 450 meV feature as the dipole active O-H stretch, the 83 meV feature as the dipole active Ni-O-H bending motion in the symmetry plane, and the 34 meV feature as the dipole active OH translational mode within the symmetry plane. The feature at 65 meV must then correspond to the dipole active Ni-OH stretch, representing only a small shift from the frequency observed for the Ni-O stretch [26,33]. On Pt(111) a similar small frequency shift has been observed for hydrogenation of Pt-O [1,2]. We can not observe or unambiguously identify the two non-dipole active modes, which are expected to have significantly less intensity.

To further exclude other possible origins for our spectral features, we finally consider other O and H containing molecules and groups. We do not observe any feature around 106 meV, which is reported to be the O-O stretch mode for hydrogen polyoxides molecules [40,41]. Thus the formation of species in our experiments, e.g. HO_2 and H_2O_2 is not supported by our EELS data in 5.2C. Due to a lack of other potential intermediates, we conclude that the frequencies observed in trace 5.2C are due to the formation of OH from annealing H_2O and O on Ni(111) above 170 K. The continued formation of H_2O from this surface to much higher temperatures in TPD experiments implies that these hydroxyl fragments recombine to form H_2O which, above 170 K, immediately desorbs.

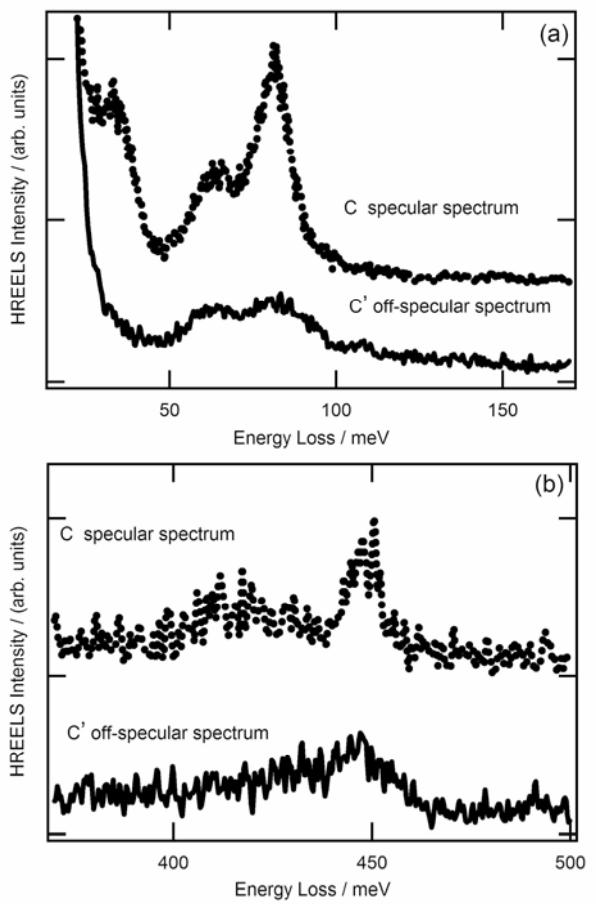

Figure 5.3 Off-specular (C') and specular (C) HREEL spectra in the range of a) 10 to 175 meV and b) 370 to 500 meV of ~1 ML H_2O co-adsorbed with ~0.05 ML atomic oxygen on Ni(111), followed by annealing to 170 K.

5.3.3 Hydroxyl co-adsorbed with water

Figure 5.4 shows HREEL spectra for the O-H stretching region for OH and H_2O under various conditions. Note that we use non-alphabetical numbering in this graph. Traces 5.4A and 5.4C are parts of the same spectra shown in figure 5.2 as traces 5.2A and 5.2C. For trace 5.4E, the Ni(111) crystal is first covered by ~ 1.1 ML H_2O at 85 K before exposing the front of the sample to 20 eV electrons for 100 s. After electron bombardment, a HREEL spectrum is recorded at 85 K. For trace 5.4F, the same treatment is applied, but after

exposure to electrons, we anneal the sample at 170 K for 100 s prior to acquiring the HREEL spectrum at 85 K.

Two features are observable in trace 5.4E: a broad feature centered at 420 meV and a sharp peak at 450 meV. As we noted before, impact of energetic electrons on adsorbed water has been shown to lead to dissociation and formation of hydroxyl species on various surfaces. The appearance of the 450 meV peak in trace 5.4E confirms that the same occurs on Ni(111). The 420 meV feature is most likely due to water molecules remaining on the surface after exposure the electrons, indicating that electron bombardment has only fragmented a fraction of the initially adsorbed water molecules. The absence of the broad feature at 420 meV in trace 4F confirms this assignment, since annealing the sample to 170 K for 100 s leads to complete desorption of molecularly-bound H_2O. The remaining feature at 450 meV in trace 5.4F results from adsorbed OH that has not yet reacted back to form H_2O.

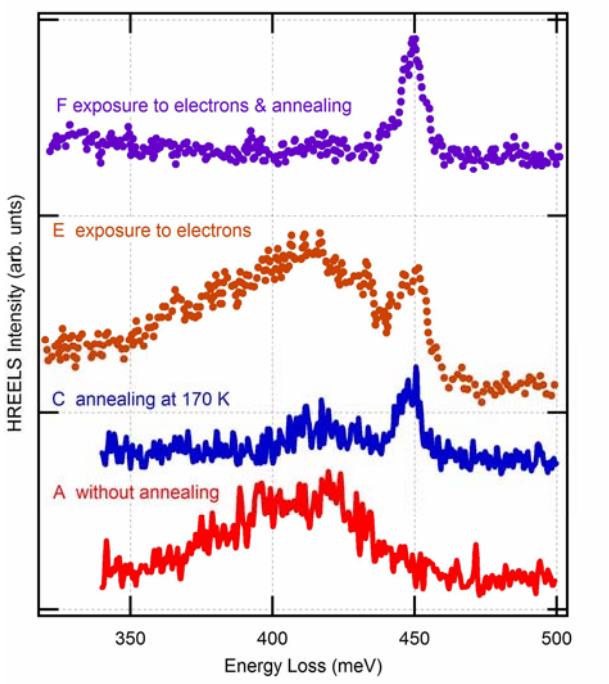

Figure 5.4 HREEL spectra of the O-H stretching range for OH and H_2O adsorbed on Ni(111) under various conditions.

Interestingly, the presence of water on the surface seems not to affect co-adsorbed OH. As discussed, OH in trace 5.4F is produced by exposure of a pure water layer to electrons, while in trace 5.4C it is produced by annealing H_2O + O to 170 K. In the latter case, very little water remains on the surface, whereas in the first case the OH is immersed in a layer of water, which we can remove by an additional annealing step. Comparing the energy loss of the hydroxyl's O-H stretching mode in traces 5.4C, 5.4E and 5.4F, we find that the center frequency and width are not affected by the presence water or the procedure employed to produce OH. We find this noteworthy for two reasons. First, the lack of change in this energy loss suggests that, even in the presence of ~1 ML of water, OH_{ads} is not involved in a hydrogen-bonded network of water molecules. Participation in such a network would have affected the O-H stretch frequency and width significantly. In addition, for Pt(111), the procedure for producing OH has been suggested to affect observed vibrational features. For OH on Ni(111) this is clearly not the case and OH can be identified unambiguously by a single set of frequencies.

The tendency of OH to participate in a hydrogen-bonded network or lack there-of may be related to the adsorption geometry of OH on the surface. For Pt(111), OH is suggested to bond with the O-H axis tilted toward to the surface on top sites [1-3]. In various relative concentrations to H_2O on Pt(111), LEED experiments suggest that OH simply replaces H_2O in hexagonal structures, creating a hydrogen-deficient water network. The deficiencies are present as missing H atoms above or below the network plane [42,43]. On Ni(111), the first water layer does wet the metal, as it does on Pt(111) [44,45], but the water structure is significantly different [27]. It has been suggested that differences are, at least in part, caused by the smaller lattice constant of Ni. Also, theoretical studies for OH on Ni(111) suggest that bonding of hydroxyl is more stable on three-fold hollow sites than on top or other sites [7,9,21]. The bond energy is calculated to be 8 times larger that the bond energy of H_2O to this surface (~80 vs. 10 kJ/mol) [7], and the O-H axis is predicted to be slightly tilted from the surface normal when adsorbed in absence of water. A continued preference for this bonding geometry in the presence of water would explain our observed results since this geometry does not allow for participation in hydrogen-bond networks which are oriented more parallel to the surface. The large bond energy of OH on the three-fold hollow site

strengthens this suggestion, since it significantly exceeds energies generally associated with hydrogen bond formation.

5.4 Conclusions

Based on HREEL and TPD spectra we identify the adsorbed hydroxyl species on the Ni(111) surface. Annealing of water on atomic oxygen pre-covered Ni(111) at 170 K or exposure of electrons to pure water on Ni(111) both lead to the hydroxyl formation. Recombination of hydroxyl is observed from ~ 180 K to ~ 240 K, leaving O_{ads} on the surface. The lack of a dependence of the O-H stretching mode to co-adsorbed water suggests that there is no hydrogen-bonding between OH and H_2O. This is in agreement with the prediction of an almost vertically bound OH on Ni(111).

5.5 References

[1] G. B. Fisher, and B. A. Sexton, *Phys. Rev. Lett.,* 1980, **44**, 683.

[2] K. Bedurftig, S. Volkening, Y. Wang, J. Wintterlin, K. Jacobi, and G. Ertl, *J. Chem. Phys.,* 1999, **111**, 11147.

[3] A. P. Seitsonen, Y. Zhu, K. Bedurftig, and H. Over, *J. Am. Chem. Soc.,* 2001,**123**, 7347.

[4] G. E. Mitchell, and J. M. White, *Chem. Phys. Lett*., 1987, **135**, 84.

[5] T. A. Germer, and W. Ho, *Chem. Phys. Lett*., 1989, **163**, 449.

[6] T. E. Madey, and F. P. Netzer, *Surf. Sci*., 1982, **117**, 549.

[7] H. Yang, and J. L. Whitten, *Surf. Sci*., 1989, **223**, 131.

[8] C. D. Roux, H. Bu, and J. W. Rabalais, *Surf. Sci*., 1992, **279**, 1.

[9] H. Yang, and J. L. Whitten, *Surf. Sci*., 1997, **370**, 136.

[10] M. Nakamura, M. Tanaka, M. Ito, and O. Sakata, *J. Chem. Phys.,* 2005, **122**, 224703.

[11] P. A. Thiel, and T. E. Madey, *Surf. Sci. Rep.,* 1987, **7**, 211.

[12] M. A. Henderson, *Surf. Sci. Rep.,* 2002, **46**, 5.

[13] G. Gilarowski, W. Erley, and H. Ibach, *Surf. Sci*., 1996, **351**, 156.

[14] E. M. Stuve, S. W. Jorgensen, and R. J. Madix, *Surf. Sci*., 1984, **146**, 179.

[15] H. Ibach, H. Wagner, and D. Bruchmann, *Solid State Commun.,* 1982. **42**, 457.

[16] L. Ollé, M. Salmeron, and A. M Baró, *J. Vacuum Sci. Technol. A,* 1985, **3**, 1866.

[17] M. Hock, U. Seip, I. Bassignana, K. Wagemann, and J. Küppers, *Surf. Sci., 1*986, **177**, L978.

[18] T. Pache, H.-P. Steinruck, W. Huber, and D. Menzel, *Surf. Sci*., 1989, **224**, 195.

[19] R. H. Stulen, and P. A. Thiel, *Surf. Sci*., 1985, **157**, 99.

[20] M. Schulze, R. Reißner, K. Bolwin, and W. Kuch, Fresenius. *J. Anal. Chem.*, 1995, **353**, 661.

[21] M. Pozzo, G. Carlini, R. Rosei, and D. Alfè, *J. Chem. Phys.,* 2007, **126**, 164706.

[22] C. T. Campbell, and S. M. Valone, *J. Vac. Sci. Technol. A,* 1985, **3**, 408.

[23] J. Shan, J. F. M. Aarts, A. W. Kleyn, and L. B. F. Juurlink, *Phys. Chem. Chem. Phys.,* 2008, **10**, 4994; this thesis chapter 4.

[24] K. Wandelt, *Surf. Sci. Rep.,* 1982, **2**, 1.

[25] P. H. Holloway, and J. B. Hudson, *Surf. Sci*., 1974, **43**, 141.

[26] G. T. Tyuliev, and K. L. Kostov, *Phys. Rev.* B, 1999, **60**, 2900.

[27] M. E. Gallagher, S. Haq, A. Omer, and A. Hodgson, *Surf. Sci*., 2007, **601**, 268.

[28] J. Shan, J. F. M. Aarts, A. W. Kleyn, and L. B. F. Juurlink, *Phys. Chem. Chem. Phys.,* 2008, **10**, 2227; this thesis chapter 3.

[29] T. Harb, W. Kedzierski, and J. W. McConkey, *J. Chem. Phys.,* 2001, **115**, 5507.

[30] C. D. Lane, N. G. Petrik, T. M. Orlando, and G. A. Kimmel, *J. Phys. Chem. C,* 2007, **111**, 16319.

[31] J. Fusy, and R. Ducros, *Surf. Sci*., 1990, **237**, 53.

[32] J. W. He, and P. R. Norton, *Surf. Sci*., 1990, **238**, 95.

[33] G. Chiarello, A. Cupolillo, C. Giallombardo, R. G. Agostino, V. Formoso, D. Pacile, L. Papagno, and E. Colavita, *Surf. Sci*., 2003, **536**, 33.

[34] M. Nakamura, and M. Ito, *Chem. Phys. Lett.,* 2004, **384**, 256.

[35] K. Jacobi, K. Bedurftig, Y. Wang, and G. Ertl, *Surf. Sci*., 2001, **472**, 9.

[36] M. W. Urban, *Vibrational Spectroscopy of Molecules and Macromolecules on Surface.* 1993, Wiley Inc, New York, p. 138.

[37] C. Klünker, C. Steimer, J. B. Hannon, M. Giesen, and H. Ibach. *Surf. Sci*., 1999, **420**, 25.

[38] R. Baddour-Hadjean, F. Fillaux, and J. Tomkinson, *Physica. B,* 1995, **213&214**, 637.

[39] H. Ibach, and D. L. Mills, *Electron Energy Loss Spectroscopy and surface vibrations.* 1982, Academic Press, New York.

[40] J. L. Arnau, and P. Giguère, *J. Chem. Phys.,* 1974, **60**, 270.

[41] C. F. Jackels, *J. Chem. Phys.,* 1993, **99**, 5768.

[42] C. Clay, S. Haq, and A. Hodgson, *Phys. Rev. Lett.,* 2004, **92**, 046102.

[43] G. Zimbitas, M. E. Gallagher, G. R. Darling, and A. Hodgson, *J. Chem. Phys.,* 2008, **128**, 074701.

[44] G. A. Kimmel, N. G. Petrik, Z. Dohnálek, and B. D. Kay, *Phys. Rev. Lett.,* 2005, **95**, 166102.

[45] G. Zimbitas, and A. Hodgson, *Chem. Phys. Lett.,* 2006, **417**, 1.